

06.1;13.1;15.2

## Features of macroscopic charge transfer in the ensembles of close-packed anatase nanoparticles near the percolation threshold

© D.A. Zimnyakov, S.S. Volchkov, A.S. Varezchnikov, M.Yu. Vasilkov, I.A. Plugin

Gagarin Saratov State Technical University, Saratov, Russia  
E-mail: zimnykov@mail.ru

Received November 7, 2022

Revised November 7, 2022

Accepted January 10, 2023

The results of experimental studies of the effect of degradation of macroscopic charge transport in ensembles of close-packed anatase nanoparticles under long-term action of a constant electric field are presented. The degradation is presumably due to the increasing degree of blocking of statistically independent conduction channels formed in ensembles of particles under the field action. A phenomenological model is considered for estimating the number of active conduction channels in an ensemble of particles near the percolation threshold in the system.

**Keywords:** nanoparticles, anatase, charge transfer, percolation threshold.

DOI: 10.21883/TPL.2023.03.55687.19414

Semiconductor nanoparticle-based structures are often used at present to fabricate chemiresistive sensors (see, e.g., [1–3]). Studies of the process of charge transfer in disordered ensembles of such nanoparticles have practical implications and also provide an opportunity to refine certain aspects of the percolation theory (see, e.g., [4–7]). Processes governing the dynamics of carriers in individual particles and border regions between them affect the macroscopic conductivity of particle ensembles. The results of examination of interrelations between microscopic and macroscopic carrier transport may be applied in the development of novel methods for research into the properties of semiconductor-based nanostructured media.

Owing to its unique properties, titanium dioxide in the anatase modification holds a special place among semiconductor materials. Anatase is a wide-band ( $E_g \approx 3.2$  eV)  $n$ -type semiconductor. According to various estimates (see, e.g., [8]), the density of mobile electrons in thin anatase films should fall within the interval from  $\sim 8 \cdot 10^{16}$  to  $9 \cdot 10^{19}$  cm $^{-3}$ . The strong interaction of mobile electrons with the lattice stipulates the polaron nature of conduction, and a high density of defects in the nanophase translates into a high probability of actuation of hopping carrier transport and the localization of carriers by traps.

Although a considerable number of papers focused on the specifics of the electron structure and various aspects of charge transport both in bulk anatase and in the nanophase have already been published, the features of carrier dynamics in ensembles of close-packed anatase particles under the influence of an electric field in near-critical conduction regimes remain understudied. In view of this, the present study is aimed at examining experimentally the dynamics of degradation of macroscopic carrier transport in such systems under long-term influence of an electric field and interpreting the obtained results in light of the concepts of gradual reduction of the number of active conduction

channels, which form in nanoparticle ensembles under the influence of an external field, with time.

The studied samples were fabricated by depositing anatase particles from aqueous suspensions onto the surface of SiO $_2$  substrates (with an interdigital system of platinum electrodes) with subsequent evaporation of the liquid phase. The interelectrode distance and the electrode width were  $\sim 90$   $\mu$ m, and the thickness of electrodes was 0.9  $\mu$ m. Zones covered by the electrode systems were  $\sim 6.9 \times 3.9$  mm in size. In the process of fabrication, the central regions of zones were coated with 8  $\mu$ l of an aqueous suspension of anatase particles (product No. 637254, Sigma Aldrich, United States;  $\langle d \rangle \leq 25$  nm; volume fraction of particles in the suspension,  $\sim 1.3 \cdot 10^{-7}$ ). The coated regions had a near-elliptical shape, and their area was  $\sim 10.1$  mm $^2$ . As water evaporated, a considerable share of particles shifted gradually from the centers of coated regions to their edges, forming peripheral structures with a high volume fraction of particles. Annular systems of „bridges“ of close-packed nanoparticles in contact with electrodes formed as a result (Fig. 1, *a*). According to AFM data (an Agilent 5600LS atomic force microscope was used), the height of „bridges“ varied from 200 to 300 nm, and their width fell within the range from 20 to 50  $\mu$ m.

Constant current  $I$  from a stabilized SRS CS-580 source was passed through the samples in experiments. The voltage drop across the samples was measured with a Keithley DAQ-6510 meter (the sampling rate was 50 Hz). Dependences  $U(t)$  of the voltage drop across the samples were recorded at  $I = 1.0$  nA and a constant temperature ( $T = 298$  K). Voltage  $U(t) = 20.0$  V was the threshold above which the SRS CS-580 source switched to the  $U$  stabilization mode. Figure 1, *b* shows the typical  $U(t)$  dependence for as-prepared samples (curve 1). Dependence  $U(t)$  for the same sample in the next measurement cycle (performed 90 min after the completion of the first

cycle) is also shown for comparison (curve 2). Curve 3 represents fluctuation component  $\tilde{U}(t) = U(t) - U_W(t)$  for dependence 1, where  $U_W(t)$  is the trend isolated by determining an autoregressive moving average with window width  $W = 160$  s. Dependence 1 features three sections: formation of a conduction structure in the sample (I) (see the inset in Fig. 1, b), quasi-steady mode (II), and nonsteady behavior of  $U(t)$ , which is characterized by considerable fluctuations and the dominance of bias current  $I_d \propto dU/dt$  in the net current through the sample (III).

Sample spectral density  $S_t(\omega)$  of fluctuation component  $\tilde{U}(t)$  at different moments  $t$  was calculated for fragments of the  $\tilde{U}(t)$  sequence 100 s in length, which were isolated by a rectangular sliding window. The sample mean frequency of fluctuations  $\bar{\omega}(t)$  was calculated next:

$$\bar{\omega}(t) = \frac{\int_{0.01 \text{ Hz}}^{25 \text{ Hz}} \omega S_t(\omega) d\omega}{\int_{0.01 \text{ Hz}}^{25 \text{ Hz}} S_t(\omega) d\omega}. \quad (1)$$

Figure 2 presents the  $\bar{\omega}(t)$  and  $\sigma_{\tilde{U}}(t)$  dependences, where  $\sigma_{\tilde{U}}$  are sample mean-square values of the fluctuation component, smoothed by median filtering.

The following phenomenological model was used to interpret the observed features of behavior of  $U(t)$ : the conduction current is produced in a sample due to the formation of a large number ( $N_{pc}$ ) of statistically independent conduction channels („percolation clusters“) within this sample. Each channel is a random chain of contacting anatase nanoparticles that supports the transfer of mobile carriers. An ensemble of channels is nonsteady due to blocking of a certain fraction of channels or emergence of new channels at arbitrary points in time. The resistance of a channel ensemble is defined as  $R_{ef} = \langle R_{pc} \rangle / N_{pc}$ , where  $\langle R_{pc} \rangle$  is the ensemble-average channel resistance. If we assume that  $\langle R_{pc} \rangle$  varies slowly, fluctuations  $\tilde{U}(t)$  are induced by the fluctuations of  $N_{pc}$ , which give rise to an additional contribution of bias current  $C_{ef}(dU/dt)$  to the net current, where  $C_{ef}$  is the effective sample capacitance.

At the initial time, the sample does not contain a formed channel ensemble. The initial  $U(t)$  section (see the inset in Fig. 1, b) suggests that an ensemble forms within  $\Delta t_f \approx 60$  s. At  $t > \Delta t_f$ , the quasi-steady mode of charge transfer, which is accompanied by a slow  $N_{pc}$  reduction due to depletion of an ensemble of mobile carriers in the sample and blocking of a fraction of nodes in channels (associated with contact zones between particles), persists through to  $t \approx 2000$  s. The value of  $C_{ef}$  also increases due to spatial separation of charges in particles.

The following relation between variations of parameters characterizing the process of charge transport holds true if the net current in a particle ensemble is constant:

$$\delta I = 0 = \delta \left[ N_{pc}(t) U(t) / \langle R_{pc}(t) \rangle \right] + \delta \left[ C_{ef}(t) \{ dU(t) / dt \} \right]. \quad (2)$$

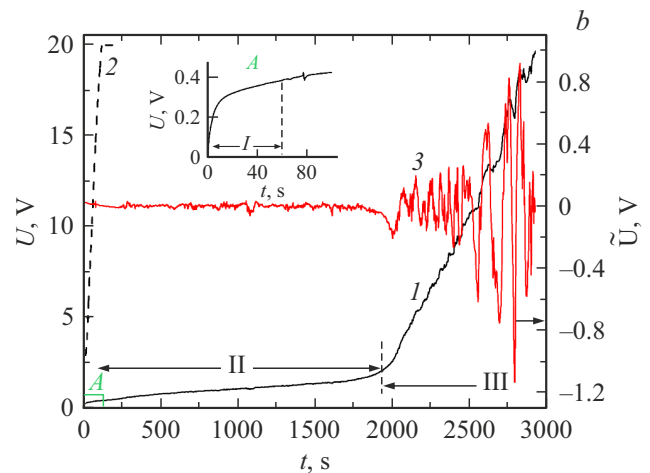
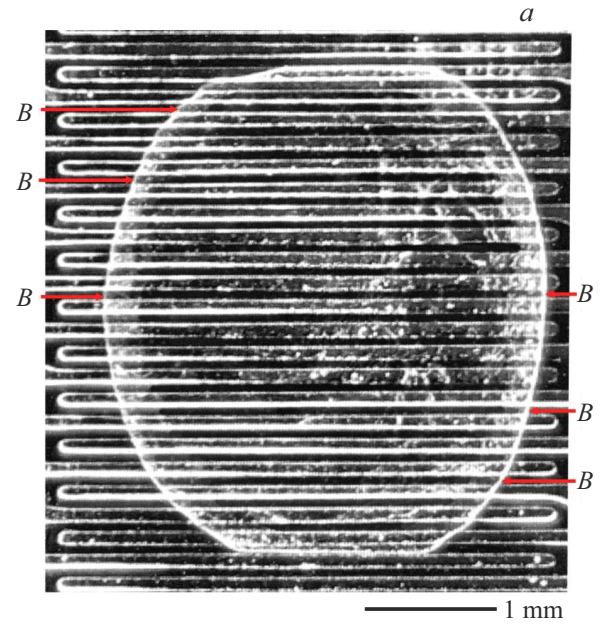


**Figure 1.** a — Macrophotographic image of a section of the interdigital electrode system with a conducting structure made of anatase nanoparticles deposited onto the surface. Letters B with arrows denote select „bridges“ between heteropolar electrodes with a high nanoparticle packing density. b — Time dependences of the current voltage drop across the sample in the first (1) and the second (2) measurement cycles and the fluctuation component of the voltage drop in the first cycle (3). The initial section of dependence  $U(t)$  in the first measurement cycle is presented in the inset.

Let us examine (2) for time intervals  $\Delta T$  wherein the variations of integral characteristics of a layer are negligible:  $\langle R_{pc}(t) \rangle \approx \text{const}$ ,  $C_{ef}(t) \approx \text{const}$ ,  $\overline{U(t)} = (1/T) \int_t^{t+T} U(t) dt \approx \text{const}$ . Assuming that the fluctuations of  $U(t)$  are induced by random variations of the number of channels, we find

$$\delta N_{pc} / N_{pc} = -(1/U) [\delta U + (\langle R_{pc} \rangle C_{ef} / N_{pc}) \delta (dU/dt)]. \quad (3)$$

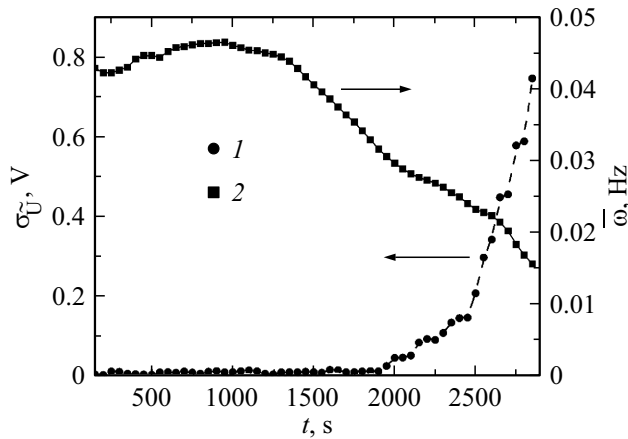


**Figure 2.** Time dependences of the sample mean-square value of the fluctuation component of the voltage drop (1) and the sample mean frequency of fluctuations (2) in the first cycle of measurements.

Parameter  $\langle R_{pc} \rangle C_{ef} / N_{pc} = R_{ef} C_{ef}$  specifies characteristic time  $\tau$  of charge transfer in an ensemble. Let us assume that  $\tau$  correlates with the mean time of fluctuations  $\bar{U}(t)$ :  $\tau \approx 2\pi / \bar{\omega}$ . The expression in square brackets on the right-hand side of (3) is the sum of random quantities: fluctuations of  $U$  and fluctuations of  $dU/dt$  scaled by parameter  $R_{ef} C_{ef}$ . Having analyzed sample experimental data, we found that the Pearson coefficient of correlation between  $\delta U$  and  $\delta(dU/dt)$  is low; therefore, the sum on the right-hand side of (3) is regarded as a sum of statistically independent quantities. Let us introduce parameter  $J$  that is specified by sample mean-square values of fluctuations of  $U$ ,  $dU/dt$  and sample-average  $\bar{\omega}$  values:

$$J = (1/\bar{U}) \sqrt{\left( \sigma_{\bar{U}}^2 + \{ (2\pi/\bar{\omega}) \sigma_{dU/dt} \}^2 \right)}. \quad (4)$$

If conduction channels are assumed to be statistically independent,

$$\delta N_{pc} / N_{pc} \propto \sigma_{N_{pc}} / \langle N_{pc} \rangle \approx \langle N_{pc} \rangle^{-0.5},$$

where  $\langle N_{pc} \rangle$  is the mean number of active channels. Thus,  $\langle N_{pc} \rangle \propto 1/J^2$ . Figure 3, *a* presents the  $J^{-2}(t)$  dependence that was reconstructed based on experimental data and reveals the transition to the percolation threshold in the studied samples.

The behavior of various parameters near the threshold should be characterized by power-law dependences of the  $(\Delta p)^\gamma$  form, where  $\Delta p$  is the detuning of a parameter from the critical value and  $\gamma$  is the critical exponent of power [9]. The near-threshold behavior of a ratio of two parameters is also characterized presumably by a power law with a certain critical exponent. Figure 3, *b* illustrates the interrelation between  $J^{-2}$  and  $\tau$ , which may be presented, with a reasonable degree of accuracy, in the form of  $\tau \propto J^{-1.161}$  at stage III. This result agrees with the conclusion of the percolation theory regarding a power divergence of the

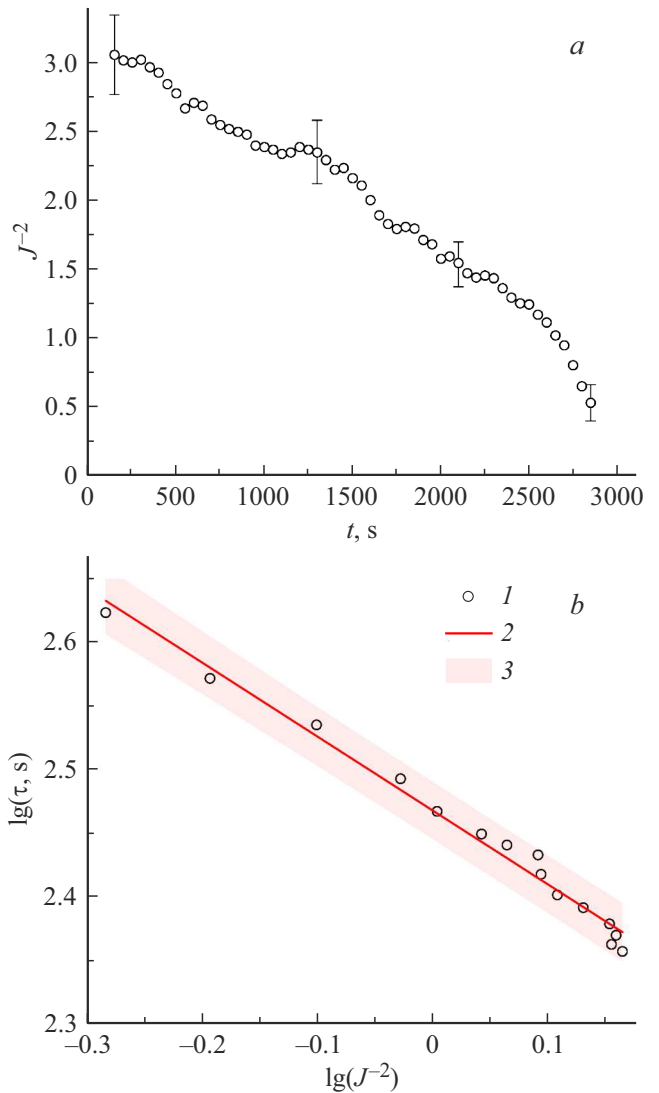


**Figure 3.** *a* — Variation of sample values of parameter  $J^{-2}$ , which were reconstructed based on experimental data and illustrate how the conducting structure approaches the percolation threshold at  $t > 2000$  s, with time. Error bars, which are indicated for select  $J^{-2}$  values, correspond to a confidence level of 0.95. *b* — Illustration of the near-power-law relation between select values of  $J^{-2}$  and  $\tau$  near the percolation threshold (for  $t > 2000$  s) (1); approximating function  $\lg \tau = 2.468 - 0.581 \lg(J^{-2})$  (2), which was obtained in accordance with the Levenberg–Marquardt procedure; and error range for a confidence level of 0.95 (3).

characteristic size of percolation clusters near the threshold (see, e.g., [10]), since  $\tau$  is defined by this size. The transition from „active“ conduction (small  $U(t)$  changes, stage II) to the „capacitive“ ( $dU_W/dt \approx \text{const}$ , stage III) mode is presumably induced by the depletion of a collective of mobile carriers in samples due to their localization at traps. This leads to an increase in the number of blocked interparticle nodes in conduction channels.

Note that the rate of relaxation of a collective of mobile carriers to the initial state (before the experiment)

at room temperature is low (curve 2 in Fig. 1, *b*; the  $dU/dt \approx \text{const}$  behavior is similar to a purely „capacitive“ one and is indicative of the lack of a well-developed system of conduction channels in the sample subjected to repeat measurements). The localization of mobile carriers at traps in anatase nanoparticles affects not only the conduction in a constant field, which was discussed in the present study, but also the optical properties of isolated nanoparticles under pulse-periodic laser irradiation in the fundamental absorption band [11]. Such irradiation induces the transition from a „semiconductor“ mechanism of radiation–particle interaction to a „dielectric“ one.

### Funding

This study was supported financially by the Russian Science Foundation (grant No. 22-29-00612).

### Conflict of interest

The authors declare that they have no conflict of interest.

### References

- [1] S.T. Navale, Z. Yang, C. Liu, P. Cao, V.B. Patil, N.S. Ramgir, R.S. Mane, F.J. Stadler, *Sensors Actuators B*, **255** (2), 1701 (2018). DOI: 10.1016/j.snb.2017.08.186
- [2] G.J. Thangamani, S.K. Khadheer Pasha, *Chemosphere*, **275**, 129960 (2021). DOI: 10.1016/j.chemosphere.2021.129960
- [3] P. Kaushik, M. Eliáš, J. Michaličková, D. Hegemann, Z. Pytlíček, D. Nečas, L. Zajíčková, *Surf. Coat. Technol.*, **370**, 235 (2019). DOI: 10.1016/j.surfcoat.2019.04.031
- [4] I.Y. Forero-Sandoval, A.P. Franco-Bacca, F. Cervantes-Álvarez, C.L. Gómez-Heredia, J.A. Ramírez-Rincón, J. Ordóñez-Miranda, J.J. Alvarado-Gil, *J. Appl. Phys.*, **131** (23), 230901 (2022). DOI: 10.1063/5.0091291
- [5] R.T. Sibatov, V.V. Uchaikin, *J. Comput. Phys.*, **293**, 409 (2015). DOI: 10.1016/j.jcp.2015.01.022
- [6] L. Qu, M. Vörös, G.T. Zimanyi, *Sci. Rep.*, **7**, 7071 (2017). DOI: 10.1038/s41598-017-06497-1
- [7] S. De, J. Coleman, *MRS Bull.*, **36** (10), 774 (2011). DOI: 10.1557/mrs.2011.236
- [8] M.C.K. Sellers, E.G. Seebauer, *Thin Solid Films*, **519** (7), 2103 (2011). DOI: 10.1016/j.tsf.2010.10.071
- [9] M. Schroeder, *Fractals, chaos, power laws. Minutes from an infinite paradise* (W.H. Freeman and Company, N.Y., 1991), p. 346–370.
- [10] P. Grinchuk, *Phys. Rev. E*, **75** (4), 041118 (2007). DOI: 10.1103/PhysRevE.75.041118
- [11] D.A. Zimnyakov, S.A. Yuvchenko, S.S. Volchkov, *Opt. Express*, **26** (25), 32941 (2018). DOI: 10.1364/OE.26.032941